reporting colitis directly associated with dasatinib therapy.[8] However, this may be a result of under-reporting of this condition rather than a true reflection of its prevalence.

There have been various theories postulated as to the mechanism of dasatinib-induced colitis. It has been hypothesised that dasatinib reduces immune tolerance.[6] Dasatinib interrupts the Src family kinase signalling pathway and thereby reduces the number of regulatory T cells in the bowel. In this way, dasatinib limits host natural immune tolerance to commensal intestinal microflora.[6,9] This allows commensal microflora to become pathogenic and cause the colitis that we associate with dasatinib. In our case the targeted colonic biopsies showed a primarily T cell infiltrate, with an increased CD8+:CD4+ ratio. In addition, there was a relative lack of regulatory T cells and NK cells, as evidenced by the sparsity of FOXP3 staining cells and absence of CD56 staining cells. The lack of regulatory T cells and reduced numbers of NK cells are in keeping with the presumed mechanism of dasatinib-induced colitis.

Dasatinib may cause a drug-induced, immune-mediated colitis in susceptible patients. This seems to be a result of the drug's broad inhibition of off-target kinases involved in regulatory T cell and NK cell proliferation, causing impaired immune tolerance. The mechanism of immune dysregulation appears to be different from the inflammatory bowel disease model, where FOXP3+CD4+ T cells predominate. Dasatinib-induced colitis is a relatively uncommon phenomenon and reverses with drug cessation. However, in cases of milder colitis or those with limited alternative therapeutic options, continuation of dasatinib is acceptable. We report a case of subclinical dasatinib-induced colitis, to add to the developing body of literature relating to this pathological process.

Conflicts of interest and sources of funding: The authors state that there are no conflicts of interest to disclose.

Aravind Gokul Tamilarasan[1], Peter Katelaris[1], Robin Gasiorowski[2], Ranjalee Liyanasuriya[3]

[1]Gastroenterology Department, Concord Hospital, The University of Sydney, Sydney, NSW, Australia; [2]Department of Haematology, Concord Hospital, The University of Sydney, Sydney, NSW, Australia; [3]Histopath Diagnostic Specialists, Sydney, NSW, Australia

Contact Dr Aravind Gokul Tamilarasan.
E-mail: gt_tamilarasan@hotmail.com

1. Jabbour E, Kantarjian H. Chronic myeloid leukaemia: 2018 update on diagnosis, therapy, and monitoring. *Am J Hematol* 2018; 93: 442–59.
2. Hochhaus A, Saussele S, Rosti G, *et al*. Chronic myeloid leukaemia: ESMO Clinical Practice Guidelines for diagnosis, treatment and follow-up. *Ann Oncol* 2017; 28 (Suppl 4): iv41–51.
3. Cortes JE, Saglio G, Kantarjian HM, *et al*. Final final 5-year study results of DASISION: the dasatinib versus imatinib study in treatment-naive chronic myeloid leukemia patients trial. *J Clin Oncol* 2016; 34: 2333–40.
4. Quintas-Cardama A, Kantarjian H, Ravandi F, *et al*. Bleeding diathesis in patients with chronic myelogenous leukemia receiving dasatinib therapy. *Cancer* 2009; 115: 2482–90.
5. Perdigoto D, Lopes S, Portela F, *et al*. Dasatinib-induced colitis in a patient with chronic myelogenous leukaemia. *GE Port J Gastroenterol* 2018; 25: 198–200.
6. Yim E, Choi Y-G, Nam Y-J, *et al*. Dasatinib induces severe haemorrhagic colitis in a patient with accelerated phase of chronic myelogenous leukaemia. *Korean J Intern Med* 2018; 33: 446–8.
7. Nishiwaki S, Maeda M, Yamada M, *et al*. Clinical efficacy of fecal occult blood test and colonoscopy for dasatinib-induced hemorrhagic colitis in CML patients. *Blood* 2017; 129: 126–8.
8. Shanshal M, Shakespeare A, Thirumala S, *et al*. Dasatinib-induced T-cell mediated colitis: a case report and review of the literature. *Acta Haematol* 2016; 136: 219–28.
9. Aldoss I, Gaal K, Al Malki MM, *et al*. Dasatinib-induced colitis after allogeneic stem cell transplantation for Philadelphia chromosome-positive acute lymphoblastic leukaemia. *Biol Blood Marrow Transplant* 2016; 22: 1900–6.

DOI: https://doi.org/10.1016/j.pathol.2019.07.013

Novel apolipoprotein AII mutation associated renal amyloidosis and fibrillary/immunotactoid cardiomyopathy

Sir,

We present the case of a novel apolipoprotein AII (apoAII) mutation related systemic deposition disease with both renal amyloidosis and cardiomyopathy with a fibrillary (F)/immunotactoid (IT) deposition pattern on electron microscopy (EM).

A 63-year-old man with end stage kidney disease secondary to amyloidosis was admitted to hospital for work-up prior to renal transplantation. Five years prior, an incidental finding of elevated creatinine and proteinuria had led to renal biopsy. In 2014 he had subsequent renal biopsies, which all showed similar features of amyloid deposition. On light microscopy (LM) there were amorphous, eosinophilic, extracellular deposits in the mesangium and arterial walls, which stained positively with Congo red and showed apple green birefringence under polarised light (Fig. 1A). Amyloid A immunoperoxidase (IPX) staining was positive (Biocare Medical, USA), while kappa and lambda immunoglobulin light chain IPX (Cell Marque, USA) showed no evidence of light chain restriction. EM confirmed the diagnosis of amyloid, demonstrating non-branching fibrils, randomly arranged, with a diameter of 8.7–12.0 nm (Fig. 1B). Genetic sequencing of lysozyme (exon 2), fibrinogen (exon 5), transthyretin (TTR, all coding exons) and apolipoprotein A1 (exon 3) failed to show any known or new DNA changes, which could be attributed to the diagnosis of hereditary amyloidosis. The patient was given a provisional diagnosis of amyloid AA, likely due to his recurrent, untreated gout.

Despite good control of his gout and normalisation of his serum amyloid A (SAA) protein levels with allopurinol, there was a progression of the renal impairment over the following years resulting in renal failure and the patient commencing peritoneal dialysis. During this time amyloid was detected in abdominal fat biopsies and incidentally in a transurethral resection of prostate. As the disease progressed, concern arose that the initial amyloid typing as AA may have been incorrect.

In the meantime, on the premise that the patient had amyloid AA and that the SAA was well controlled, the patient began work-up for renal transplant from a live dedicated donor.

A transthoracic echocardiogram (TTE), performed as part of his pre-transplant investigations, showed a moderate

increase in left ventricular wall thickness, mildly increased myocardial echogenicity, mild diastolic dysfunction and a heterogeneous polar map of strain measurement, which although suggestive of an infiltrative cardiomyopathy was not typical of cardiac amyloid. Contrast magnetic resonance imaging was contraindicated due to renal failure. These discrepancies on TTE findings and the knowledge that amyloid AA is rarely associated with cardiac amyloid, prompted a right ventricular biopsy.

LM of the endomyocardial biopsy showed deposition of extracellular hyaline material surrounding myocytes and nodular deposits in the subendocardium (Fig. 2A). Morphologically the appearance was suggestive of amyloid, however using the technique of Putchler (1962), Congo red stains were repeatedly negative at our institution. Subsequently, using the same staining method at the National Amyloidosis Centre in London, a positive Congo red stain was finally obtained. This demonstrated apple-green birefringence under high intensity cross polarised light. IPX staining was performed using a panel of monospecific antibodies as previously described:[1] P component (Dako, Denmark), kappa immunoglobulin light chain (Dako), lambda immunoglobulin light chain (Dako), AA (Euro Diagnostica, Sweden), lysozyme (Dako), fibrinogen alpha chain (Cambichem), apoA1 (Genzyme, USA), Lect 2 (R&D Systems, USA). Specificity of staining was confirmed by prior absorption of the antiserum with pure antigen in each case and positive and negative controls were included in each run. However, the results did not reveal a specific cause of the deposits.

EM of the endomyocardial deposits demonstrated tubular structures, ranging from 8 to 16 nm in diameter. The tubules were deposited in an organised pattern in some areas (Fig. 2B) with other areas showing a more random pattern

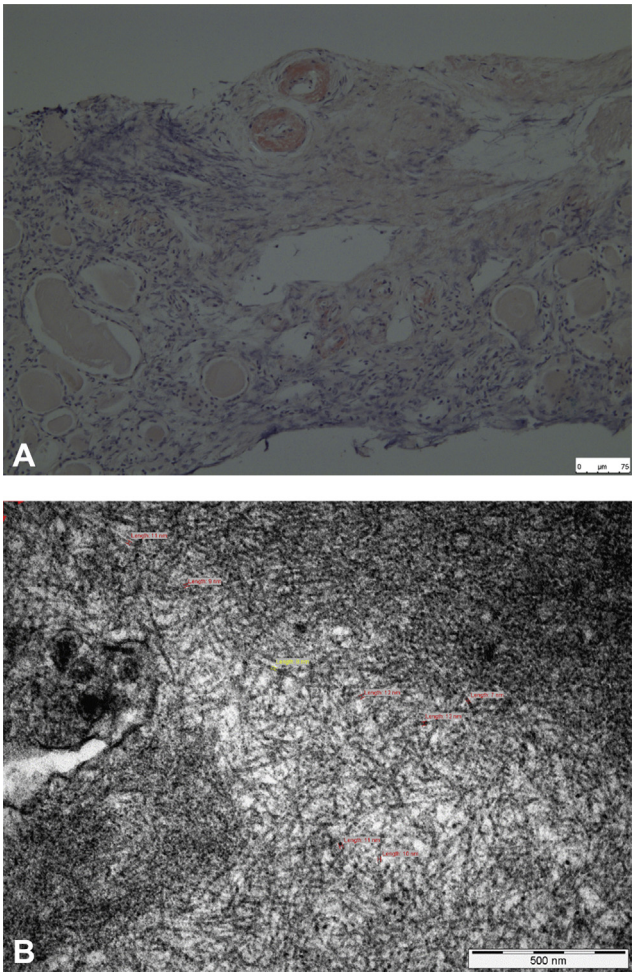

Fig. 1 Renal biopsy 2014. (A) Light microscopy: Congo red positive amyloid deposits in blood vessel walls. (B) Electron microscopy: amyloid deposits show randomly arranged fibrils.

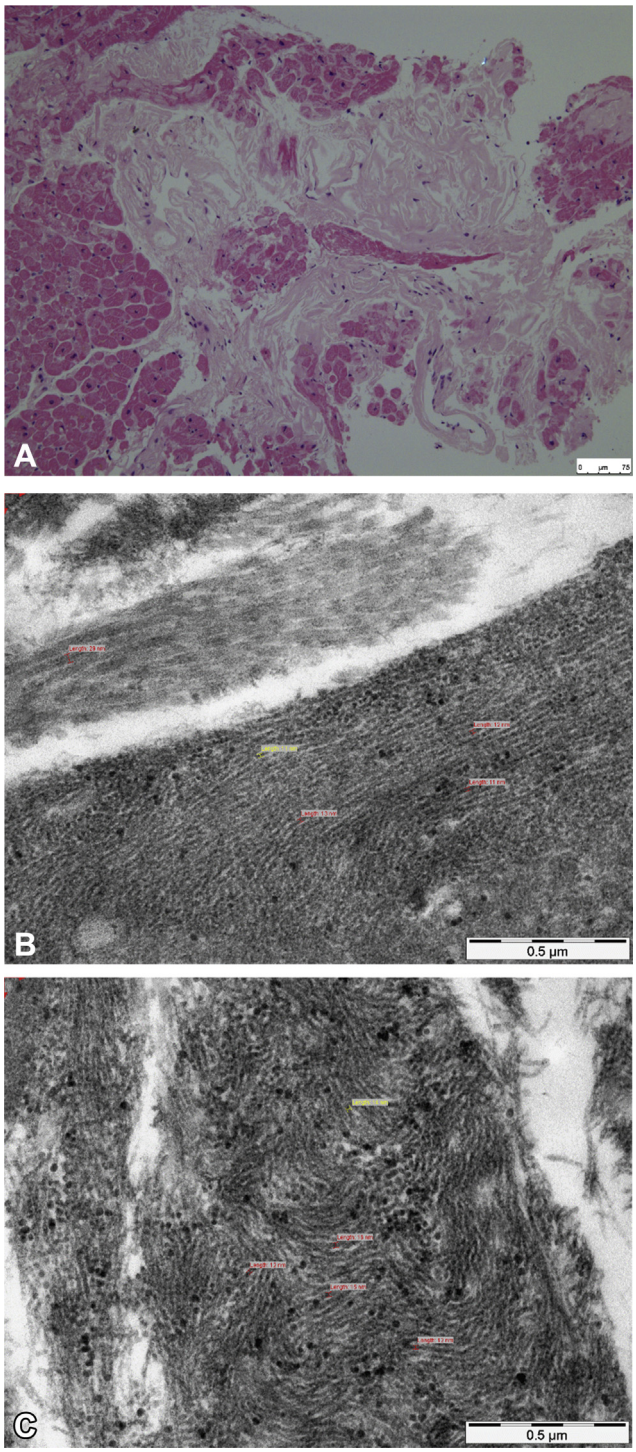

Fig. 2 Endomyocardial biopsy 2016. (A) Light microscopy shows extracellular, amorphous pink deposits. (B) Electron microscopy shows an organised arrangement of tubules and (C) more randomly arranged tubules.

(Fig. 2C). A diagnosis of F/IT deposition cardiomyopathy was made.

Mass spectrometry of the cardiac deposits undertaken at the National Amyloidosis Centre in London, detected apolipoprotein AII (apoAII, being a component of high density lipoprotein) and strongly suggested that apoAII was the main constituent, thus raising the possibility that the patient may have familial amyloidosis. Subsequent genetic analysis at the same institution revealed a novel substitution, c.298A>C, in the *APOA2* gene. There was no mutation in other genes known to be associated with hereditary amyloidosis including apoAI, TTR and LYZ.

The patient underwent a successful live donor renal transplant and follow-up renal biopsies 1 month post-transplant showed no evidence of recurrent disease.

Inherited apoAII amyloidosis is extremely rare and was first described in 2001.[2] It is predominantly associated with renal involvement although cardiac amyloid has also been reported. To date four mutations have been identified and all involve loss of the stop codon at residue 101, giving rise to a novel 21 amino acid peptide extension. In this case, analysis of the *APOA2* gene revealed the patient was heterozygous for the previously unreported substitution c.298A>C, which also resulted in the loss of the stop codon and a novel 21 amino acid peptide extension p.Ter101Cys*21. This mutation, along with the mass spectrometry finding of a predominance of apoAII, support the pathogenicity of the novel *APOA2* gene substitution in this patient. The fibrils identified in the renal biopsies and the microtubules in the cardiac biopsy are both thought to consist of variant apoAII protein. Unfortunately there was insufficient renal tissue remaining for mass spectrometry to confirm this hypothesis and there is no commercially available IPX for apoAII.

Amyloid, fibrillary and IT deposition belong to a family of diseases with the same underlying cause, i.e., they are all due to the extracellular deposition of insoluble proteins. These conditions are most commonly described in the kidney and are classified largely based on their LM and ultrastructural characteristics.[3,4] Amyloid deposits are classically confirmed by positive Congo red staining on LM, with apple green birefringence under polarised light. EM examination of amyloid fibrils shows non-branching, randomly arranged fibrils ranging from 8−12 nm in diameter. Systemic amyloidosis has been well described in the kidney and the heart, and both organs are not uncommonly affected simultaneously. In fact, amyloid cardiomyopathy is the leading cause of death in immunoglobulin light chain amyloidosis (AL).[5]

However, F/IT deposition cardiomyopathy is a very rare condition with only one previously reported case.[6] Although F and IT deposition have traditionally been described together, there is evidence to suggest that they can be divided into two entities, largely based on studies of renal disease where they are more often encountered. Both F and IT deposition classically do not stain with Congo red and are distinguished from each other by their ultrastructure. The EM of fibrillary deposition shows randomly arranged fibrils, 15−30 nm in diameter. In glomerular disease, fibrillary deposition is uncommonly associated with an underlying lymphoplasmacytic disorder or gammopathy (only 5%) and has a poor prognosis with 44% developing chronic renal failure within 24 months.[3,4] In contrast, the EM of IT deposition shows microtubules in an organised, often parallel arrangement and a larger, 10−90 nm diameter. Renal IT deposition is more commonly associated with an underlying lymphoplasmacytic disorder or gammopathy and has a better prognosis than fibrillary glomerulopathy.[4]

Thus, separating F and IT deposition is thought to be of diagnostic and prognostic relevance in renal disease. Whether this can be translated to cardiac deposition disease remains to be studied. In this case, the endomyocardial deposits showed somewhat confusing and overlapping features. Unlike amyloid, they were repeatedly negative to Congo red staining at our institution, however they subsequently showed positive Congo red staining and apple green birefringence at the National Amyloid Centre UK. Although Congophilia is traditionally associated with amyloid, recent cases of Congophilic fibrillary glomerulonephritis (which also display birefringence under polarised light), have been published.[7] Similarly, the ultrastructural properties displayed some overlap between F and IT deposits, i.e., both an organised arrangement in keeping with IT and a more random distribution in keeping with F in other areas. The size of the tubules was also at the smaller end of the range for IT and was more in keeping with F or amyloid sizing. Thus, the final diagnosis of F/IT cardiomyopathy was made. The presence of cardiac F/IT deposits and their unusual Congo red staining properties may be a feature of this novel apoAII mutation.

The single previous case report of fibrillary/immunotactoid cardiomyopathy occurred in a 44-year-old woman with chronic renal failure also due to F/IT deposition.[6] The EM findings were reported as randomly arranged fibrils 8.0−12.4 nm in diameter, as opposed to an organised arrangement of tubules 8−16 nm in diameter in this case. In fact, the previous report may have been better classified as fibrillary deposits, emphasising the unique nature of our case.

This case highlights the clinical and pathological features of a newly described hereditary apoAII mutation which the evidence strongly suggests has caused both amyloid and F/IT disease. In practice, however, hereditary amyloidoses are rarely diagnosed, with AL, AA and ATTR accounting for nearly 90% of systemic amyloidosis.[8] Identifying this novel genetic cause is significant, as previous study has shown that apoAII amyloidoses have a high incidence of cardiac involvement[9] and there are potential ramifications for other family members if the mutation is germline. We have shown a novel apoAII mutation which is associated with both systemic amyloidosis (in particular with renal disease) and with a unique cardiomyopathy that has features of several different types of deposition, i.e., the Congo red staining properties of amyloid and a subset of fibrillary, with the ultrastructure of both fibrillary and immunotactoid disease.

Acknowledgements: Levina Dear, Acting Head of Department, The Electron Microscopy Unit, ICPMR Westmead Hospital, NSW, Australia; Carol Robinson, Technical officer, The Electron Microscopy Unit, ICPMR Westmead Hospital, NSW, Australia; Anita Achan, Pathologist, ICPMR, Westmead Hospital, NSW, Australia; Janet A. Gilbertson, University College, London, UK.

Conflicts of interest and sources of funding: The authors state that there are no conflicts of interest to disclose.

Joanne Brown[1], Siddharth Trivedi[2,3], Fiona Kwok[4], Dorota Rowczenio[5], Liza Thomas[2,3], Winny Varikatt[1,3]

[1]Tissue Pathology and Diagnostic Oncology, Institute of Clinical Pathology and Medical Research, Westmead Hospital, Westmead, NSW, Australia; [2]Department of Cardiology, Westmead Hospital, Westmead, NSW, Australia; [3]Westmead Clinical School, Faculty of Medicine and Health, The University of Sydney, Sydney, NSW, Australia; [4]Department of Clinical Haematology, Westmead Hospital, Westmead, NSW, Australia; [5]National Amyloidosis Centre, University College Medical School, London, United Kingdom

Contact Dr Winny Varikatt.
E-mail: Winny.Varikatt@health.nsw.gov.au

1. Roweczenio D, Stensland M, de Souza GA, *et al*. Renal amyloidosis associated with 5 novel variants in the fibrinogen A alpha chain protein. *Kidney Int Rep* 2016; 2: 461−9.
2. Benson MD, Liepnieks JJ, Yazaki M, *et al*. A new human hereditary amyloidosis: the result of a stop codon mutation in the apolipoprotein AII gene. *Genomics* 2001; 72: 272−7.
3. Joh K. Pathology of glomerular deposition disease. *Pathol Int* 2007; 57: 551−65.
4. Herrera G, Turbat-Herrera E. Renal diseases with organized deposits: an algorithmic approach to classification and clinicopathological diagnosis. *Arch Pathol Lab Med* 2010; 134: 512−53.
5. Badar T, Cornelison A, Shah N, *et al*. Outcome of patients with systemic light chain amyloidosis with concurrent renal and cardiac involvement. *Eur J Haematol* 2016; 97: 342−7.
6. Sabatine M, Aretz T, Fang L, *et al*. Fibrillary/immunotactoid glomerulopathy with cardiac involvement. *Circulation* 2002; 105: e120−1.
7. Alexander M, Dasari S, Vrana J, *et al*. Congophilic fibrillary glomerulonephritis: a case series. *Am J Kidney Dis* 2018; 72: 325−36.
8. Vrana J, Gamez J, Madden B, *et al*. Classification of amyloidosis by laser microdissection and mass spectrometry-based proteomic analysis in clinical biopsy specimens. *Blood* 2009; 114: 4957−9.
9. Benson MD, Kalopissis AD, Charbert M, *et al*. A transgenic mouse model of human systemic ApoA2 amyloidosis. *Amyloid* 2011; 18 (Suppl 1): 32−3.

DOI: https://doi.org/10.1016/j.pathol.2019.07.011

Reactive lymphadenopathy with concurrent idiopathic plasma cell variant Castleman disease, amyloid deposition and non-caseating granulomas

Sir,

Amyloid lymphadenopathy is characterised histologically by effacement of the nodal architecture by eosinophilic amorphous material that exhibits apple-green birefringence with Congo red stain examined in cross-polarised light. The pattern of effacement can be diffuse, involve follicles predominantly (i.e., follicular), or a combination of follicular and diffuse. Immunoglobulin-derived light chain amyloidosis (AL amyloid) is most common. A recent report of 47 cases found that 39 were systemic and four localised AL amyloid, whereas only one case each was AA (serum amyloid A protein), wtTTR (wild type transthyretin), V122ITTR (transthyretin V122I).[1] The identification of AL amyloid is often suggestive of plasma cell dyscrasia, idiopathic amyloidosis or a lymphoproliferative neoplasm. AA amyloid, sometimes referred to as secondary amyloidosis, is often associated with reactive conditions including autoimmune diseases and infectious aetiologies.[2] Due to a persistent chronic inflammatory state, lymph nodes can be complicated by the deposition of serum amyloid A protein (SAA) and development of secondary amyloidosis. Here, we present a patient with lymphadenopathy attributable to idiopathic plasma cell variant Castleman disease, amyloid deposition, and non-caseating granulomas.

A 62-year-old human immunodeficiency virus (HIV)-negative African American woman presented with dysphagia and fatigue. She had a history of diabetes type II, hypothyroidism, Plummer−Vinson syndrome and persistent lymphadenopathy of the porta hepatis. Five years prior to this visit, the patient had a needle core biopsy of an enlarged portal lymph node that revealed scattered secondary follicles with an increased number of small mature-appearing plasma cells in the interfollicular areas. Some follicles showed small, lymphocyte-depleted germinal centres. No amyloid was identified. No aberrant B or T cells were identified by flow cytometry immunophenotypic analysis. Molecular studies using polymerase chain reaction (PCR)-based methods show no evidence of monoclonal *IGH* or *TRG* or *TRB* rearrangements. A diagnosis of plasma cell variant Castleman disease was suggested.

For the current visit, laboratory studies showed moderate microcytic anaemia with a haemoglobin level of 7.6 g/dL [reference range (RR) 12.0−16.0 g/dL] and MCV of 65 fl (RR 82−92 fl). In addition, increased free kappa (115 mg/L; RR 3.3−19.4 mg/L) and lambda light chain (78 mg/L; RR 5.7−26.3 mg/L) were present with a normal kappa/lambda ratio of 1.46 (RR 0.26−1.65). A computed tomography (CT) scan of the abdomen showed lymphadenopathy: a 2 cm supra-pancreatic lymph node, a 2 cm hepatic artery lymph node, and a 5 cm porta hepatis lymph node that were stable compared to the imaging studies performed 5 years previously. No other enlarged lymph nodes were identified. Foci of calcified granulomas were detected in the liver, spleen and right lung base. The patient underwent an excisional biopsy of portal and supra-pancreatic lymph nodes. Histological examination revealed enlarged lymph nodes with patent sinuses and variably sized follicles scattered in the cortex and medulla (Fig. 1A−D). Many follicles showed deposits of amorphous eosinophilic material in the centres of the follicles and some showed mantle zone hyperplasia with an 'onion-skin' appearance (Fig. 1E,F). The interfollicular regions and medulla were occupied by sheets of cytologically mature plasma cells. Vascular proliferation was present in the interfollicular areas and occasional hyalinised blood vessels penetrating follicles (hyaline-vascular lesions) were present (Fig. 1G,H). In addition, focal distinct non-caseating granulomas containing rare giant cells and asteroid bodies were present (Fig. 1K,L). Special stains were performed to characterise the eosinophilic deposits and non-caseating granulomas. Congo-red stain demonstrated apple-green birefringence in areas with eosinophilic deposits (Fig. 1I,J,M,N,O). AFB was negative for acid-fast bacilli and GMS was negative for fungal organisms. Immunohistochemistry (IHC) for IgG4 highlighted <10% of IgG+ plasma cells. HHV8 stain was negative. Flow cytometry analysis showed no aberrant B or T cells and polytypic plasma cells.